

1                   **Atlantic modulation of El Niño influence on summertime rainfall**  
2   **over Southeastern South America**

3  
4   **Marcelo Barreiro**

5   Unidad de Ciencias de la Atmósfera, Facultad de Ciencias, Universidad de la República, Montevideo,  
6   Uruguay

7   **Andrés Tippmann**

8   Instituto de Mecánica de Fluidos e Ingeniería Ambiental, Facultad de Ingeniería, Universidad de la  
9   República, Montevideo, Uruguay

10  
11  
12   *Corresponding author address:* Marcelo Barreiro, Unidad de Ciencias de la Atmósfera, Instituto de  
13   Física, Facultad de Ciencias, Universidad de la República, Igua 4225, Montevideo 11100, Uruguay.

14                   Tel: +5982 5258624, Fax: +5982 5250580, Email: [barreiro@fisica.edu.uy](mailto:barreiro@fisica.edu.uy)

## Abstract

15  
16 This study addresses the effect of Atlantic sea surface temperature (SST) anomalies on rainfall over  
17 southeastern South America during January-February, particularly during El Niño years, using  
18 observations as well as model simulations. It is found that the state of the equatorial Atlantic during El  
19 Niño years can modulate its influence on rainfall over southeastern South America, such that when the  
20 equatorial Atlantic is warm, the El Niño influence is weaker. This Atlantic influence is shown to occur  
21 through the response of the low level winds to equatorial SST anomalies: the convergence of westerly  
22 anomalies onto the warm anomaly decreases the equatorial trades and moisture flow into the Amazon  
23 and, moreover, reduces the northerly flow that brings moisture to southeastern South America. The  
24 total rainfall response in this region can thus be thought as the combination of rainfall anomalies from  
25 the equatorial Pacific and Atlantic oceans.

## 26 **1. Introduction**

27 Southeastern South America (SESA, here defined as the region [65°W-47°W,19°S-37°S]) is one of the  
28 regions of the world most influenced by El Niño [e.g Ropelewski and Halpert, 1987, 1989; Pisciottano  
29 et al, 1994]: a warm SST anomaly in the equatorial Pacific induces a tendency for higher precipitations.  
30 The influence depends on the season, with largest signal during spring of the El Niño years, tends to  
31 weaken during January-February (JF) of the following year, and then strengthens again in March  
32 [Pisciottano et al, 1994; Cazes-Boezio et al, 2003]. Here we focus on El Niño influence in high summer  
33 (JF) to determine what factors may induce the observed inter-event variability. The La Niña influence  
34 on SESA during summer is even less clear [Pisciottano et al, 1994; Silvestri, 2004] and is not  
35 considered here.

36 The mechanisms through which El Niño influences SESA involve both upper and lower level  
37 atmospheric circulation anomalies. During El Niño the strengthening and meandering of the subtropical  
38 jet in upper levels due to Rossby wave trains propagating from the equatorial Pacific increases  
39 baroclinicity and the advection of cyclonic vorticity over SESA. In lower levels the northerly flow from  
40 the Amazon basin strengthens increasing the availability of moisture south of 20°S [Silvestri, 2004].  
41 Both conditions favor the increase in precipitation for a canonical El Niño in spring. During high  
42 summer, however, the subtropical jet moves poleward weakening the upper level mechanism [Cazes-  
43 Boezio et al, 2003].

44 Even though there is a tendency to rain more there is significant variability in the influence of El Niños  
45 on precipitation over SESA during JF. It has been recently proposed for February-March that some of  
46 the differences in this influence lies in the strength of El Niño [Silvestri, 2004]. According to this study  
47 only strong events induce the wave trains in upper levels that propagate toward South America  
48 enhancing the subtropical jet at about 30°S. On the other hand, Barros and Silvestri [2002] and Vera et  
49 al [2004] pointed out the importance of SST variations in the south central Pacific in modulating the  
50 influence of El Niño events during spring over SESA. They find that the influence is larger if the

51 equatorial Pacific SST anomalies has a different sign than the SST anomalies in the south central  
52 Pacific.

53 In this work we study, using observations and model simulations, the possibility that the state of the  
54 tropical Atlantic during El Niño events induces inter-El Niño differences in the rainfall anomalies over  
55 SESA. Among others, Giannini et al [2004] and Chang et al [2006] have pointed out the importance of  
56 the preconditioning of the tropical Atlantic in the response of this basin to the remote El Niño  
57 influence. Moreover, it has been shown that increased rainfall over SESA is associated with a  
58 strengthened Low-Level Jet [e.g. Doyle and Barros, 2002]. Since low level winds respond to equatorial  
59 SST it is possible that equatorial Atlantic anomalies change the low level flow that brings moisture  
60 from the Amazon to SESA, strengthening/weakening the anomaly induced by the Pacific. Here we  
61 show that this is indeed the case: El Niño events that coincide with a warm equatorial Atlantic tend to  
62 induce smaller rainfall anomalies over SESA than those events that coincide with negative or neutral  
63 conditions in the Atlantic.

64

## 65 **2. Observed El Niño influence over SESA and the state of the equatorial Atlantic**

66 We use winds and moisture fields from the NCEP-NCAR Reanalysis CDAS-1 (originally on a  
67  $2.5^\circ \times 2.5^\circ$  grid) that are interpolated onto the same horizontal grid as the Speedy model (see section 3).  
68 The SST data set is that of ERSSTv.2, also with the same resolution as Speedy. We use the PREC-L  
69 data set of Chen et al [2002] for land precipitation. This rainfall product is based on gauge observations  
70 from the Global Historical Climate Network, regridded on a  $2.5^\circ \times 2.5^\circ$  grid. El Niño years are defined  
71 as those years in which the SST anomaly in the region Niño3.4 during December-January is larger than  
72 1 K, with December corresponding to the previous year we considered the anomalies over SESA. This  
73 definition was used in Giannini et al [2007], but differs from others usually used (e.g. Trenberth  
74 [1997]). Neutral years are those in which the absolute value of SST anomalies in the region Niño3.4 are  
75 less than 1 K. Throughout this work we considered the period from January 1949 to December 2006.

76 During summertime there are two preferential paths of moisture fluxes to the northern border of SESA:  
77 one from the south Atlantic at about 15-20°S, and one from the equatorial Atlantic that flows west to  
78 the Amazon basin and is then funneled south by the Low Level Jet [Doyle and Barros, 2002; Soares  
79 and Marengo, 2006]. Note that in the latter path, part of the moisture evaporated in the equatorial  
80 Atlantic will not reach SESA because of rainout upstream [Vimeux et al, 2005]. Thus, the moisture  
81 flow into SESA may vary due to the strength of the winds (particularly of the Low Level Jet) and/or  
82 due to the upstream availability of moisture. To characterize the flow in this latter path we define an  
83 index (ZI) as the mean 850 mb zonal winds over the western equatorial Atlantic ([60°W-20°W,5°S-  
84 5°N]). The wind stress over this region was used by Chang et al [2006] to characterize the interaction  
85 between Pacific El Niño and the Atlantic Niño. We show below that when this equatorial flow  
86 increases (ZI<0), there is enhanced moisture transport into SESA that leads to an increase in rainfall  
87 there, as humidity is the main limiting factor for rainfall in this region [Doyle and Barros 2002].  
88 As mentioned in the introduction the influence of El Niño on SESA, although significant, is relatively  
89 weak during JF (Figures 1a,d). The composites of El Niño events stratified according to ZI show that  
90 even though there is a tendency to rain in both cases, the anomalies are much larger and statistically  
91 significant only for the composite of El Niño years that have easterly anomalies (negative ZI) in the  
92 region off the Amazon (compare Figures 1b,c). The SST composites of these two groups of El Niños  
93 reveal that the case with positive/negative ZI has large/weak SST anomalies in the equatorial Atlantic  
94 (Figure 1e,f). Note that Atlantic SST anomalies in the composite for ZI>0 are about 0.5-0.6 K, larger  
95 than the SST standard deviation during JF. Furthermore, the composite of 850mb moisture flux for the  
96 case ZI<0 shows significant easterly anomalies bringing additional moisture to the Amazon that tends  
97 to be afterward funneled southward by the Low Level Jet resulting in a positive surface moisture  
98 (precipitable water) anomaly in SESA (Figures 2b,d). In the composite for ZI>0 there is an anticyclonic  
99 anomaly centered at about (55°W,10°S) that advects moisture to the north of SESA but not into the  
100 region resulting in a tendency for moisture deficit in the southern part of SESA (Figure 2a,c).

101 These results suggest the existence of a mechanism through which the equatorial Atlantic can influence  
102 rainfall over SESA and modulate the El Niño influence. Nevertheless, the use of observations alone  
103 does not allow to separate other possible reasons for the observed difference in rainfall response  
104 between the different El Niños. For example, though of similar spatial structure, the composite for  
105  $ZI>0$  has smaller SST anomalies in the equatorial Pacific than the case for  $ZI<0$ , and thus the strength  
106 of the El Niño event may play a role. To address these issues we turn to simulations with an  
107 atmospheric general circulation model forced with historical SST.

108

### 109 **3. Model simulations**

110 The model used in this study is Speedy, a full atmospheric model with simplified physics and an  
111 horizontal resolution of T31 ( $3.75^\circ \times 3.75^\circ$ ) with 8 vertical levels [Molteni 2003; Kucharski et al 2005].  
112 The model has a bias consisting in a maximum of summer rainfall in the western part of SESA, instead  
113 of a more uniform observed rainfall distribution [Kucharski et al 2005]. This bias is also reflected in the  
114 precipitation anomalies. For example, for El Niño years the simulated anomalies are centered at about  
115 ( $60^\circ\text{W}$ ,  $24^\circ\text{S}$ ) instead of at about ( $55^\circ\text{W}$ ,  $28^\circ\text{S}$ ) as shown in Figure 1a (not shown).

116 We performed 3 experiments in order to separate the influence of SST anomalies in different basins on  
117 rainfall over SESA: GOGA (Global Ocean-Global Atmosphere), where the model is forced with global  
118 historical SST, and POGA/AOGA where the model is forced with historical SST only in the  
119 Pacific/Atlantic basin between  $50^\circ\text{S}$ - $30^\circ\text{N}$  and climatological SST is prescribed elsewhere. We  
120 considered the same period as observations, and constructed an ensemble of 10 runs for each  
121 experiment. Results are based on the ensemble mean for each experiment during the months of JF.

122 Figure 3 shows the composites of horizontal moisture advection at 850mb for the three experiments  
123 during El Niño years stratified according to the observed ZI (that is, the equivalent maps to those in  
124 Figures 2a,b). A decomposition of the changes in moisture advection due to humidity and wind  
125 anomalies reveals that the moisture transport anomalies of Figure 3 are mainly due to changes in the

126 circulation. The effect of El Niño on the moisture flux can be readily seen in the composites for POGA  
127 (Figures 3b,e). Both panels show increased easterly flux toward the Amazon basin in equatorial region  
128 (in agreement with Chang et al [2006]) and a strengthening in the northerly moisture transport from the  
129 Amazon into the SESA region. Moreover, the larger anomalies in the composite for  $ZI < 0$  shows that  
130 the strength of El Niño is an important player in generating inter-event variability during JF [cf.  
131 Silvestri 2004]. Comparison of composites for GOGA and POGA experiments reveals that the Atlantic  
132 ocean plays an important role in changing this Pacific influence. For example, in the composite for  
133  $ZI > 0$  GOGA shows westerly flux anomalies on the equatorial Atlantic, the opposite from POGA, and  
134 weaker northerly flow into SESA. These differences can be reconciled using the results of the AOGA  
135 experiment. In the latter, the warm equatorial Atlantic (case  $ZI > 0$ ) induces westerly equatorial moisture  
136 flux anomalies due to wind convergence onto the positive SST anomaly and southerly transport  
137 anomalies between 10-20°S that tend to decrease the moisture flux from the Amazon to SESA, both  
138 changes opposing the influence from the Pacific. Consequently, for El Niño years with  $ZI > 0$  the  
139 precipitation over SESA is the result of increased rainfall due to El Niño and decreased rainfall due to a  
140 warm equatorial Atlantic. Indeed, the composite of precipitation anomalies associated with the upper  
141 panels of Figure 3 show that the average rainfall over SESA in GOGA= +0.03 mm day<sup>-1</sup>, in POGA=  
142 +0.21 mm day<sup>-1</sup>, and in AOGA= -0.18 mm day<sup>-1</sup>, suggesting a linear response to the equatorial Pacific  
143 and Atlantic oceans.

144 For El Niño years with  $ZI < 0$  the AOGA experiment shows weak 850mb moisture transport anomalies,  
145 as expected due to small equatorial Atlantic SST anomalies. Nevertheless, even small changes in  
146 Atlantic SST are able to significantly reduce the Pacific influence over the that basin as can be seen  
147 from the comparison between the POGA and GOGA composites of moisture flux (Figures 3d,e).

148 Lastly, we show that the proposed mechanism is actually the one that induces the extreme rainfall  
149 anomalies in SESA during neutral (not El Niño nor La Niña) years. To do so we considered the years  
150 of extreme rainfall over SESA in AOGA that do not coincide with El Niño or La Niña years and

151 constructed the composite of atmospheric anomalies for positive minus negative cases (Figure 4).  
152 Consistent with our previous findings the composite shows that negative SST anomalies in the  
153 equatorial Atlantic force positive rainfall anomalies over SESA due to increased northerly moisture  
154 transport at low levels into SESA. In the upper levels winds are statistically significant only over the  
155 equatorial Atlantic and correspond to the usual baroclinic response to an atmospheric cooling (not  
156 shown).

157 The pattern of SST anomaly that is related to rainfall over SESA in AOGA has its maximum in the  
158 central equatorial Atlantic region. A composite of observed rainfall anomalies during neutral years  
159 based on extremes of the ATL3 index (SST averaged over [20°W-0°E,3°S-3°N]) does not show a clear  
160 picture over SESA. This may be due to insufficient statistics (small number of cases) and/or because  
161 the Atlantic influence is relatively weak compared to internal atmospheric variability.

162

#### 163 **4. Summary**

164 The influence of El Niño during high summer in the precipitation over SESA varies considerably. As  
165 found by Silvestri [2004] for February-March using observations, we showed using model simulations  
166 that the strength of El Niño accounts for a part of the observed inter-event variability of rainfall  
167 anomalies in JF. Moreover, we propose that the equatorial Atlantic SST plays a role in modulating the  
168 El Niño signal. We found that when the equatorial Atlantic is warm the influence of El Niño over  
169 SESA is weaker than when there are no significant equatorial anomalies. Using modeling experiments  
170 we showed that a warm equatorial Atlantic induces equatorial westerlies and, most importantly,  
171 weakens the Low Level Jet that transports moisture from the Amazon to SESA, thus limiting the  
172 availability of moisture in the region. This opposes the influence of the equatorial Pacific SST, and as  
173 result, it rains less when the model is forced with global SST than when only SST anomalies in the  
174 Pacific are used. Further modeling studies are needed to test the sensitivity of the proposed mechanism  
175 to model formulation.

176 It is worth noting that the ATL3 index has maximum variance during June-August associated with the  
177 Atlantic Niño [Zebiak, 1993], and a secondary maximum in November-January associated with a  
178 different mode that is independent on the Pacific El Niño [Okumura and Xie, 2006]. Most of the  
179 studies of the equatorial Atlantic modes have focused on the austral winter season. Our results point to  
180 the importance of understanding the dynamics of the equatorial ocean-atmosphere interaction during  
181 austral summer and underscores the need for monitoring the equatorial Atlantic. A better understanding  
182 of the influence of this basin on South American climate may help improving seasonal climate  
183 prediction.

184

185 **Acknowledgments** – The authors would like to thank G. Cazes and S. Talento for their useful  
186 comments in the course of the study. This work was supported by Programa de Desarrollo  
187 Tecnológico, Uruguay.

188

## 189 **References**

190 Barros, V. R., and G. Silvestri (2002), The relationship between sea surface temperature at the  
191 subtropical south central Pacific and precipitation in southeastern South America, *J. Clim.*, *15*, 251-  
192 267.

193 Cazes-Boezio, G., A. W. Robertson, and C. R. Mechoso (2003), Seasonal dependence of ENSO  
194 teleconnections over South America and relationships with precipitation in Uruguay, *J. Clim.*, *16*,  
195 1159-1176.

196 Chang, P., Y. Fang, R. Saravanan, L. Ji, and H. Seidel (2006), The cause of the fragile relationship  
197 between the Pacific El Niño and the Atlantic Niño, *Nature*, *443*, 324-328.

198 Chen, M., P. Xie, J. E. Janowiak, and P. A. Arkin (2002), Global land precipitation: A 50-yr monthly  
199 analysis based on gauge observations, *J. of Hydrometeorology*, *3*, 249-266.

200 Doyle, M. E., and V. Barros (2002), Midsummer low-level circulation and precipitation in subtropical

201 South America and related sea surface temperature anomalies in the south Atlantic, *J. Clim.*, *15*, 3394-  
202 3410.

203 Giannini, A., R. Saravanan and P. Chang (2004), The preconditioning role of Tropical Atlantic  
204 Variability in the development of the ENSO teleconnection: implications for the prediction of Nordeste  
205 rainfall. *Clim. Dyn.*, *22*, 839-855.

206 Giannini, A., A. W. Robertson, J.-H. Qian (2007) A role for tropical atmospheric temperature  
207 adjustment to El Niño-Southern Oscillation in the seasonality of monsoonal Indonesia precipitation  
208 predictability. *J. Geophys. Res.*, *112*, D16110, doi:10.1029/2007JD008519.

209 Kucharski, F., F. Molteni, and A. Bracco (2005), Decadal interactions between the western tropical  
210 Pacific and the North Atlantic Oscillation, *Clim. Dyn.*, doi:10.1007/s00382-005-0085-5.

211 Molteni, F. (2003), Atmospheric simulations using a GCM with simplified physical parametrizations. I.  
212 Model climatology and variability in multi-decadal experiments, *Clim Dyn.*, *20*, 175-191

213 Okumura, Y, and S-P. Xie (2006), Some overlooked features of tropical Atlantic climate leading to a  
214 new Niño-like phenomenon, *J. Clim.*, *19*, 5859-5874.

215 Pisciotano, G., A. Diaz, G. Cazes, and C. R. Mechoso (1994), El Niño-Southern Oscillation impact on  
216 rainfall in Uruguay, *J. Clim.*, *7*, 1286-1302.

217 Ropelewski, C. H., and S. Halpert (1987), Global and regional scale precipitation patterns associated  
218 with the El Niño-Southern Oscillation, *Mon. Wea. Rev.*, *115*, 1606-1626.

219 Ropelewski, C. H., and S. Halpert (1987), Precipitation patterns associated with the high index phase of  
220 the Southern Oscillation, *J. Clim.*, *2*, 268-284.

221 Silvestri, G. E. (2004), El Niño signal variability in the precipitation over southeastern South America  
222 during austral summer, *Geophys. Res. Lett.*, *31*, doi:10.1029/2004GL020590.

223 Soares, W. R., and J. A. Marengo (2006), The importance of the low-level jet east of Andes on  
224 moisture transport over South America, Proceedings of 8 ICSHMO, Foz do Iguacu, Brasil, 2006, INPE  
225 1197-1202.

226 Trenberth, K. (1997), The definition of El niño, *Bull. Amer. Meteorolo. Soc.*, 78, 2771-2777.  
227 Vera, C., G. Silvestri, V. Barros, and A. Carril (2004), Differences in El Niño Response over the  
228 Southern Hemisphere, *J. Clim.*, 17, 1741-1753.  
229 Vimeux, F., R. Gallaire, S. Bony, G. Hoffmann, and J. C.-H. Chiang (2005), What are the climate  
230 controls on  $\Delta D$  in precipitation in the Zongo Valley (Bolivia)? Implications for the Illimani ice core  
231 interpretation, *Earth Planet. Sci. Lett.*, 240, 205-220.  
232 Zebiak, S. (1993), Air-sea interaction in the equatorial Atlantic region, *J. Clim.*, 6, 1567-1586.

233

### 234 **Figure Captions**

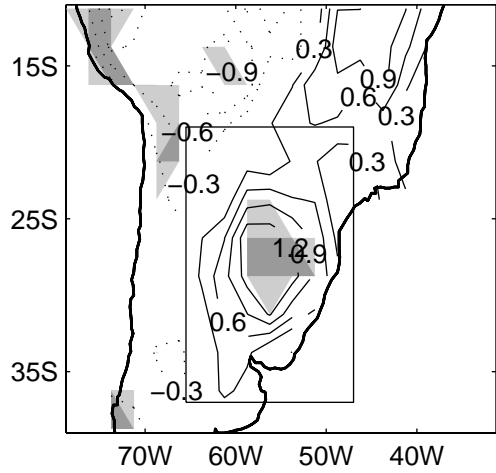
235 **Figure 1** – Composite of observed precipitation ( $\text{mm day}^{-1}$ ) and SST anomalies (K) of El Niño years  
236 versus neutral years. The leftmost panels show the composites for all El Niño years (a,d). The two other  
237 columns show the composite of El Niño events stratified according to ZI: (b,e) El Niño events that have  
238  $ZI > 0$  (westerlies off the Amazon), and (c,f) El Niño events that have  $ZI < 0$ . The light/dark shading  
239 marks the regions that are statistically significant at the 10%/5% level using a two-sided Student t-test.  
240 The box marks the SESA region.

241 **Figure 2** – Composites of observed 850 mb moisture flux and specific humidity integrated between  
242 850 and 1000 mb for the composite of El Niño years vs. neutral years stratified according to ZI. (a,c) El  
243 Niño events that have  $ZI > 0$  (same years as in Figures 1b,e); (b,d) El Niño events that have  $ZI < 0$  (same  
244 years as in Figures 1c,f). Shading and box as in Figure 1.

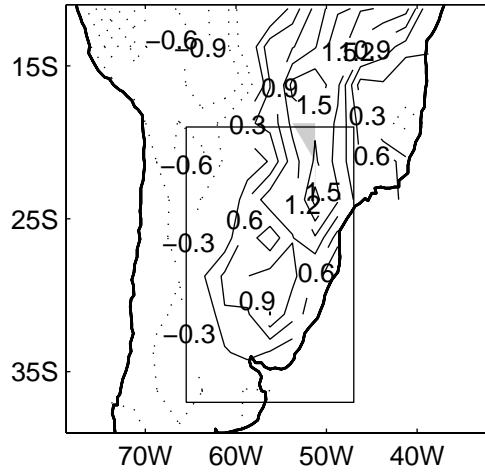
245 **Figure 3** – Composites of simulated 850 mb moisture transport for El Niño events that have  $ZI > 0$   
246 (upper panels), and for El Niño events that have  $ZI < 0$  (lower panels). Columns show the maps for  
247 GOGA (left), POGA (middle) and AOGA (right) experiments. The El Niño years in each ZI-class are  
248 the same of Figure 1. The composites are constructed as the average during stratified El Niño years  
249 minus the average of neutral years in the ensemble mean of each experiment. Shading and box as in  
250 Figure 1.

251 **Figure 4** – Composite during years of extreme rainfall (larger than one standard deviation) over SESA  
252 in the AOGA experiment that are neutral years. The composites are constructed as the average of  
253 positive minus negative extreme precipitation events. (a) Precipitation ( $\text{mm day}^{-1}$ ), (b) 850 mb moisture  
254 transport, and (c) SST (K). Shading and box as in Figure 1.

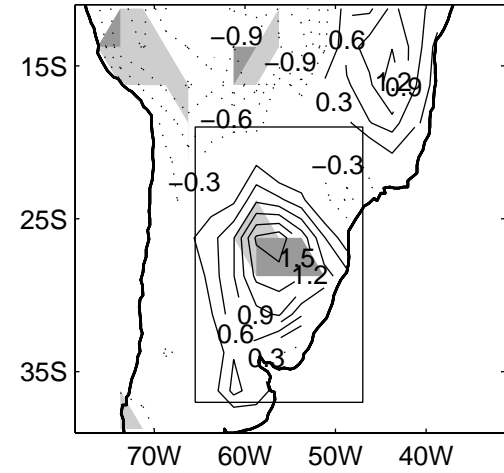
a. Nino years  
 1957 1963 1965 1968 1972  
 1982 1986 1991 1994 1997 2002



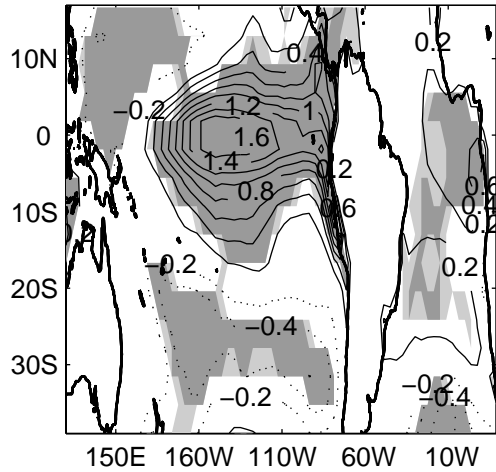
b. Nino years & ZI positive  
 1963 1994 1997 2002



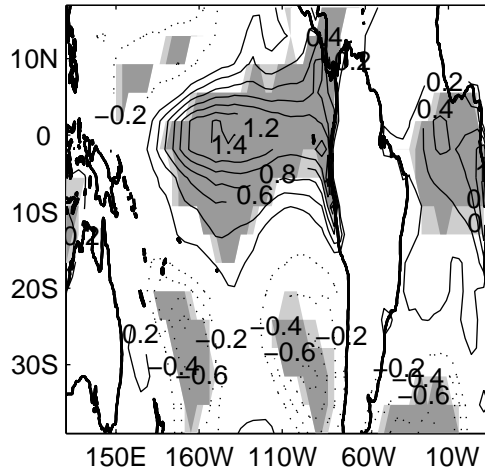
c. Nino years & ZI negative  
 1957 1965 1968 1972 1982 1986 1991



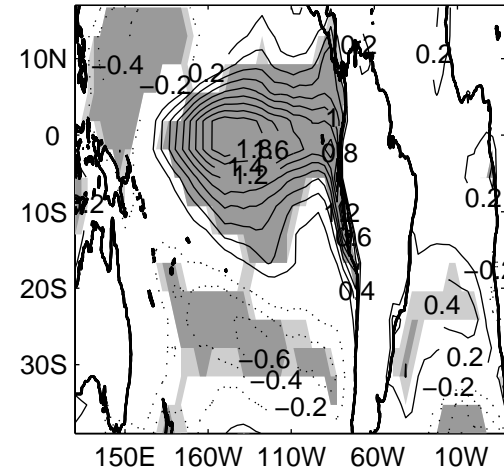
d.



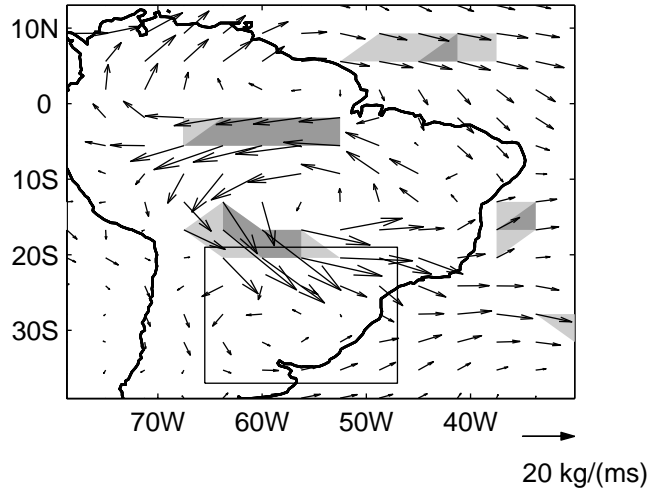
e.



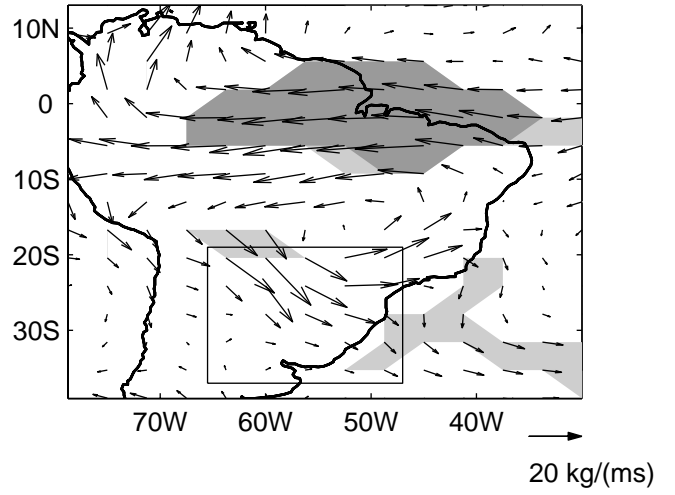
f.



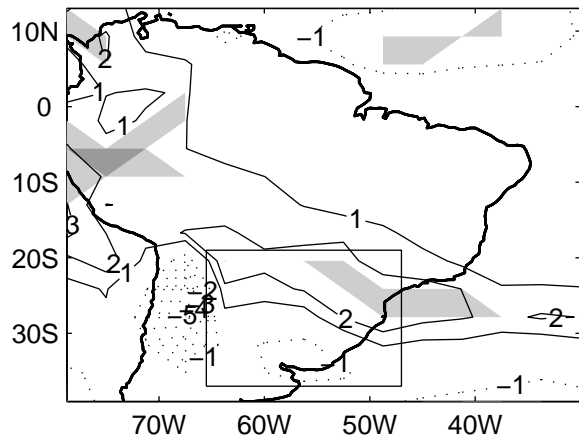
a. Nino years & ZI positive  
850mb moisture flux



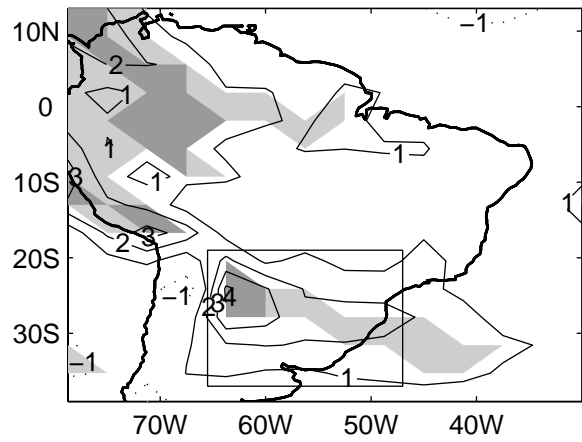
b. Nino years & ZI negative  
850mb moisture flux



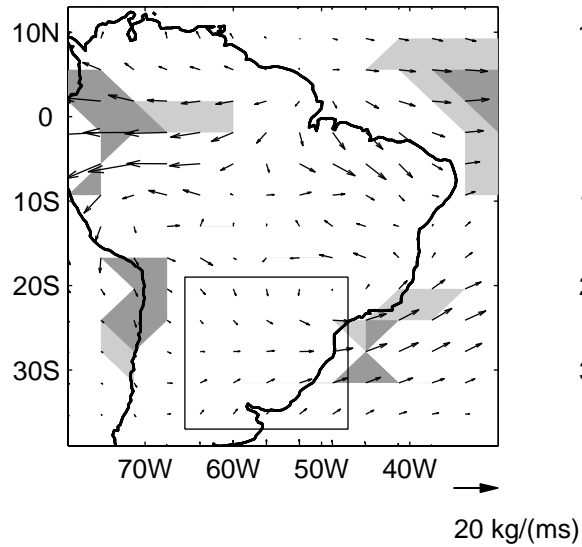
c. Moisture



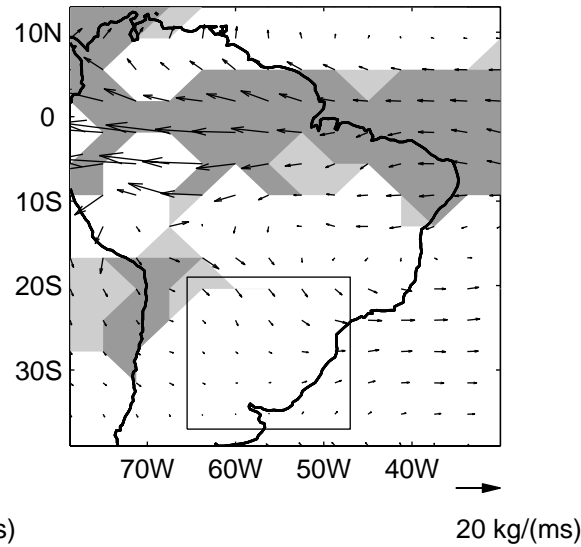
d. Moisture



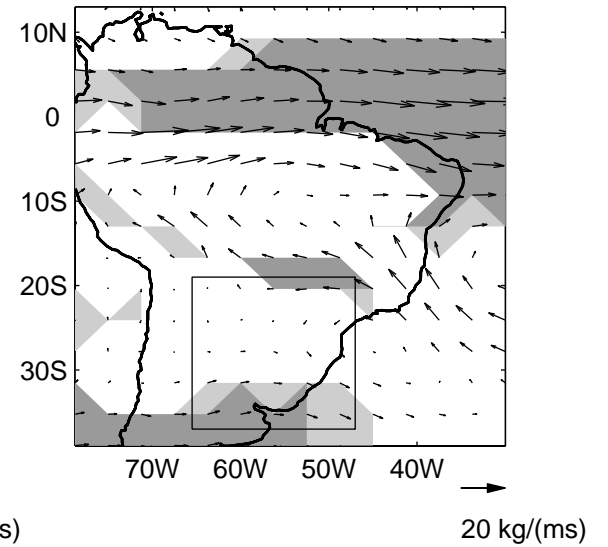
a. GOGA, Nino years & ZI positive



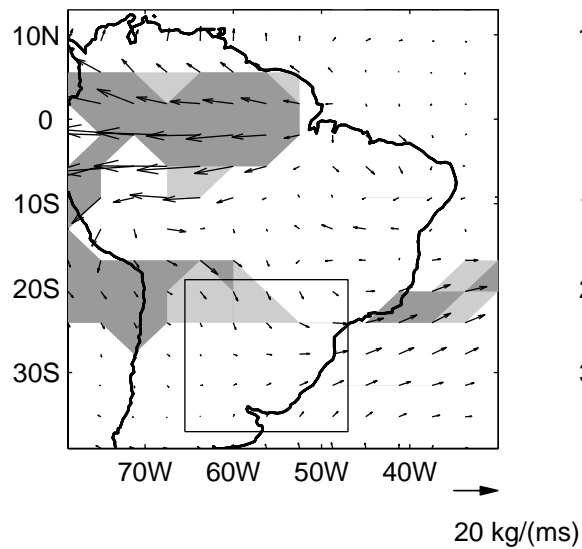
b. POGA, Nino years & ZI positive



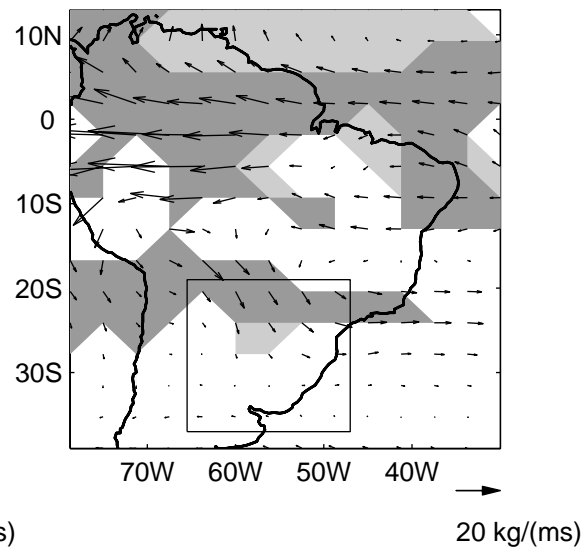
c. AOGA, Nino years & ZI positive



d. GOGA, Nino years & ZI negative



e. POGA, Nino years & ZI negative



f. AOGA, Nino years & ZI negative

